

ChemComm

Accepted Manuscript



This is an *Accepted Manuscript*, which has been through the Royal Society of Chemistry peer review process and has been accepted for publication.

Accepted Manuscripts are published online shortly after acceptance, before technical editing, formatting and proof reading. Using this free service, authors can make their results available to the community, in citable form, before we publish the edited article. We will replace this *Accepted Manuscript* with the edited and formatted *Advance Article* as soon as it is available.

You can find more information about *Accepted Manuscripts* in the [Information for Authors](#).

Please note that technical editing may introduce minor changes to the text and/or graphics, which may alter content. The journal's standard [Terms & Conditions](#) and the [Ethical guidelines](#) still apply. In no event shall the Royal Society of Chemistry be held responsible for any errors or omissions in this *Accepted Manuscript* or any consequences arising from the use of any information it contains.

COMMUNICATION

Cite this: DOI: 10.1039/x0xx00000x

Active Colloidal Microdrills

Received 00th January 2014,
Accepted 00th January 2014J. G. Gibbs^{†a,b} and P. Fischer^{a,c}

DOI: 10.1039/x0xx00000x

www.rsc.org/

We demonstrate a chemically driven, autonomous catalytic microdrill. An asymmetric distribution of catalyst causes the helical swimmer to twist while it undergoes directed propulsion. A driving torque and hydrodynamic coupling between translation and rotation at low Reynolds number leads to drill-like swimming behaviour.

Propulsion at the micro and nanoscale¹ can be achieved by a wide range of methods including the use of light,² biomolecular motors,³ acoustics,⁴ thermophoresis,⁵ enzymes,⁶ as well as electric,⁷ and magnetic fields.⁸ One of the most popular routes is chemical propulsion due to the lack of a need to introduce an external driving force. A typical system of this type is a nano⁹ or microstructure which consists of an on-board catalyst.¹⁰ This type of motor catalyzes a locally available chemical fuel and thereby gives rise to self-phoretic locomotion. In recent years, many systems of this type have been studied, and a wide range of architectures and morphologies have been demonstrated. The most common are the following: asymmetric half-coated micro *Janus* spheres,^{11, 12} bi-metallic nanorods,¹³ microjet microtubes,¹⁴ and shell motors,¹⁵ just to name a few. The listed examples are usually structurally symmetric (e.g. spherical), and the asymmetry

necessary for proper motion is primarily due to an asymmetric distribution of catalyst on the structure. However, structurally asymmetric autonomous micromotors display swimming behaviour that is not observed in their symmetrical counterparts and therefore warrant investigation.

For micromotors of complex shape, an intricate interplay between the driving force and hydrodynamic interactions exists, yet this can be advantageous. Since the shape¹⁶ and material composition of active colloidal particles dictate the type of swimming behaviour observed, desired motion characteristics can be engineered into the system if the microswimmer fabrication process can be precisely controlled. Here we show that by using a dynamic fabrication technique, we can manufacture several billion microdrills that are catalytically active and at the same time structurally anisotropic. These chemically propelled colloidal swimmers undergo coupled translational and rotational motion in a corkscrew type movement. Although the motors exhibit a range of different swimming behavior, the one we focus upon is autonomous corkscrew motion, as this is the basis of any screw or drill.

This motion is a result of simultaneous material and geometric asymmetries made possible by the fabrication process. In particular, the swimmer consists of a spherical head with a helical tail, in the shape of a corkscrew, in which both the head and the helix backbone consist of silica, SiO₂. The spherical heads in this case are 1 μm microbeads, and the helix tail is fabricated using glancing angle deposition (GLAD) which is a dynamic physical vapor deposition process.¹⁷ GLAD uses vapour incidence angles $\alpha \sim 85^\circ$. The microbeads act as seeds for the accumulation of material during GLAD growth and ensure a higher structural uniformity. By combining grazing incidence with simultaneous substrate rotation, the tail can be grown in a helical fashion.

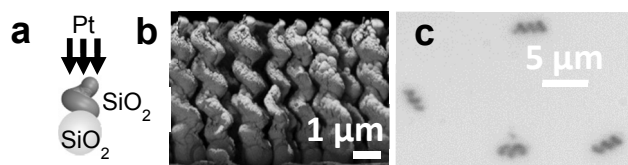


Fig. 1 (a) Schematic of the deposition process to coat one side of a helix with Pt; (b) a cross-section SEM image of the autonomous catalytic microdrills imaged after the deposition process. The Backscattered Electron (ESB) detector allows for the contrast between the SiO₂ backbone and the Pt (lighter contrast) to be clearly distinguished; (c) optical micrograph of microdrills in water (snapshot of Brownian motion).

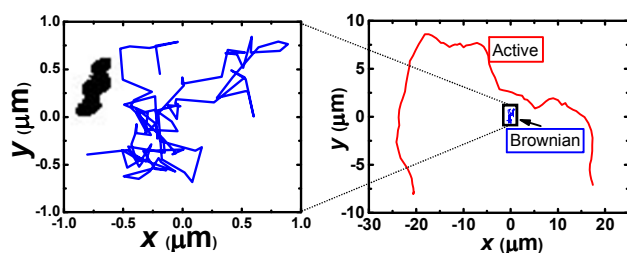


Fig. 2 Left plot: Brownian motion for a single microdrill in the absence of fuel over a 5 s interval at a frame rate of 20 fps. Inset (top left): binary image of the chemically propelled microdrill (not to scale); right plot: comparison of the same Brownian motion vs. an active particle over the same time period.

The total length of the catalytic microdrills (including the spherical head), major diameter, minor diameter, pitch (threads per length), and thread angle are $l = 4 \pm 1 \mu\text{m}$, $D = 1400 \pm 200 \text{ nm}$, $d = 630 \pm 70 \text{ nm}$, $p = 1330 \pm 80 \text{ nm}$, and $\theta = 32 \pm 5^\circ$, respectively (see electronic supplementary information, ESI). In this case, the threads of the microdrills are left-handed, dictated by the rotation sense of the substrate during the deposition. It should be noted that the variation in the total length, l , is due to the competitive growth which is typically seen in GLAD.¹⁷

Platinum (Pt), which acts as the onboard catalyst, is coated onto the structures in an asymmetric manner. This asymmetric distribution of the catalyst is critical for propulsion, as is well known. The schematic in Fig. 1 (a) shows how platinum (Pt) is deposited at a normal incidence angle, $\alpha = 0^\circ$, onto a 1-turn helix, so that Pt will only coat one side. By repeatedly growing individual single turns followed by the procedure shown in Fig. 1 (a), the resulting structures, shown in the cross-section scanning electron micrograph (SEM) image in Fig. 1(b), can be fabricated. By using an energy selective backscattered (ESB) electron detector, the contrast between the SiO_2 (darker contrast) and the Pt (lighter contrast) can be easily distinguished in the image. The details of the fabrication process, morphological characterization, and other

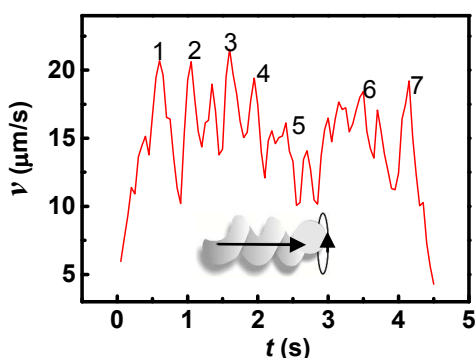


Fig. 3 speed variation of a single microdrill over ~5s. near the solid-liquid interface (corresponding to ESI video V8). Each rotation can be seen as a spike in the speed. Inset: schematic showing an individual microdrill which rotates and translates autonomously, due to the catalyzed reaction of H_2O_2 .

experimental procedures and conditions, such as particle tracking etc., can be found in the ESI.

The particles are easily separated, removed from the substrate, and suspended into a colloidal suspension by ultrasonication for ~10 s. Individual separated and removed microdrills can be seen in the optical microscope image of Fig. 1 (c) in which the particles have settled to the surface of the microscope slide. Here, they undergo effectively 2D diffusion, due to partial confinement to the surface by gravity, brought on by thermal movement of the surrounding solvent molecules. Two example videos of a single particles undergoing Brownian motion in H_2O alone can be found in the ESI. The diffusion coefficient (for a sphere) of radius R is given by $D = k_B T / 6\pi\eta R$, where $k_B T$ is the energy, and η is the fluid viscosity. The diffusion constant was determined by calculating the mean squared displacement (MSD) for five diffusing particles and was calculated to be $D = 0.35 \pm 0.01 \mu\text{m}^2/\text{s}$.

When hydrogen peroxide, H_2O_2 , is added, the motors' behavior is dramatically changed. The thin coating of Pt is sufficient to catalyze the decomposition of H_2O_2 into reaction products: O_2 and H_2O . A comparison of a single particle diffusing in H_2O vs. an active particle in H_2O with added H_2O_2 is shown in Fig. 2. A marked difference in the translational

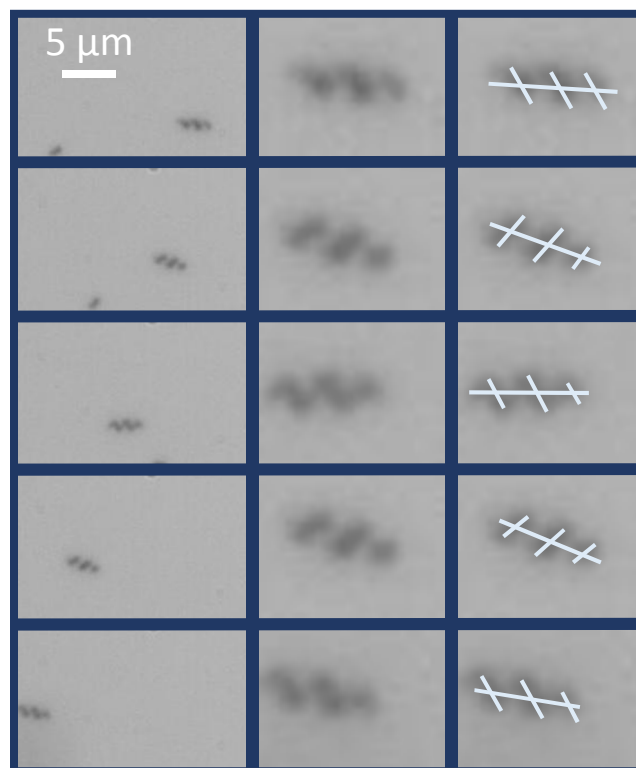


Fig. 4 Left column: video frames of a microdrill chosen so that the simultaneous translation and rotation is clearly seen ($\Delta t = 0.26, 0.21, 0.26, 0.32 \text{ s}$ between sequential frames from top to bottom). Middle column: zoomed in and centered frames of the same particle showing half-turns ($\pi \text{ rad.}$ rotations) between each frame. Right column: parallel lines are drawn to highlight the relative angle between the drill threads and the helix axis – clearly showing rotation.

movement can be seen for the same length of time, i.e. 5 s. The changes in direction are caused primarily by rotational Brownian motion.

It has been shown that typically for a system in which the autonomous swimmer consists of a catalyst on an electrically insulating material, the motor will be propelled away from this site where the reaction is occurring. The direction of propulsion for catalyst-on-insulator motors has been established^{12, 16} and suggests that the microdrills are propelled away from the catalyst site. In the ensemble of microdrills, we, however, also find a wide variety of motion behavior, such as pure translation, spinning about the helix axis while translating (microdrill motion), spinning perpendicular to the helix axis with little translation, and end-over-end rotation (tail movement side-to-side). Table S1 in the ESI summarizes the statistics for 134 swimmers chosen at random. These variations are attributed to inhomogeneity amongst both particle morphology and catalyst coating. Videos of each type of movement can also be seen in the ESI with several showing microdrill movement (~25% undergo this type of movement).

We focus our attention on this type since, to the best of our knowledge, autonomous movement of this kind has never been characterized to date, although a roughly similar structure was briefly characterized once before.¹⁸ Microdrills that are undergoing both rotational and translational movement near the solid-liquid interface display the following traits: as seen in Fig. 3, the translational speed is a function of time. The rotation rate is also directly related to translational speed as well; as the rotation rate increases, so does the translational speed. The typical behavior observed is the following: translation with slow rotation occurs for a short interval, followed by quick rotation at which time the translational speed increases. For the swimmer in Fig. 3, this cycle repeats with a periodicity of $\sim 6\pi$ rad/s. The numbers above the peaks in the example of Fig. 3 show the completion of one full rotation at which time the particle's rotation rate and translational speed again slow, then the cycle repeats. The exact nature of the speed changes is not fully understood, but observation suggests they arise due to interactions with the surface, as the microdrill exposes the catalyst towards the substrate and then away from it as it rotates.

Figure 4 details how the rotational motion is verified. The left column shows sequential frames from a video which correspond to π rad rotations. The position of the frame in this case is fixed to show translation. The center and right columns focus upon axial rotation. The Pt coating can be clearly resolved (darker color) with bright-field microscopy, allowing for the observation of the rotational orientation. The light colored lines are added in the right column to highlight the location of the Pt against the background. It can clearly be seen that the lines are tilted with respect to the helix axis by an angle corresponding to whether the exposed Pt is facing the microscope objective or pointing away from it. That is, the microdrill has made a half turn. Therefore, we conclude that the autonomous, active drill is in fact undergoing simultaneous translation and rotation.

The variation in orientation of the microdrill for each half turn, as shown in the left column of Fig. 4, suggests that the driving force is not collinear with the drill's axis, i.e. there is a lateral component to the driving force, which leads to reorientation. This effect is due to the asymmetric distribution of the Pt as is discussed in the ESI. This reorientation for each half turn can be seen clearly in several videos; for example: ESI video V11.

The motion of interest, i.e. simultaneous rotation and translation or autonomous microdrill movement, is due to two factors: first, the distribution of the Pt is asymmetric along the threads of the drill (resulting from the deposition process, as described in the ESI). The asymmetry leads not only to a reorientation, as described in the previous paragraph, but also is responsible for a driving torque, causing the microdrill to rotate along its axis. The second factor leading to this type of movement is the coupling between rotation and translation as the microdrill is propelled directionally by the driving force. The coupling between rotation and translation at low Reynolds number is described by the following 2×2 resistance matrix

$$\begin{pmatrix} F \\ \tau \end{pmatrix} = \begin{pmatrix} A_{11} & A_{12} \\ A_{21} & A_{22} \end{pmatrix} \begin{pmatrix} v \\ \omega \end{pmatrix} \quad (1)$$

in which F , τ , v , and ω are the force, torque, speed and axial rotation frequency, respectively.¹⁹ Both F and τ can be considered to be non-zero with these two observations. Each matrix element in equation (1) is dependent solely upon the shape of the particle. A driving torque alone leads to propulsion due to hydrodynamic coupling, as in the case of magnetically actuated nanopropellers. Therefore, the translational motion is enhanced by the driving torque. A full characterization of the hydrodynamics is beyond the scope of this communication.

In conclusion, we have fabricated and characterized an autonomous, catalytic microdrill which exhibits a wide variety of different swimming behaviors. We have focused our attention on microdrill swimming motion which exhibits simultaneous translation and rotation about the structure's axis. This motion arises from both the asymmetric distribution of the catalyst as well as hydrodynamic coupling between rotation and translation. We believe these results could lead to important applications, such as drilling into cells,²⁰ and will spark future studies addressing the understanding of this type of autonomous microdrill activity.

Notes and references

^a Max Planck Institute for Intelligent Systems, Heisenbergstr. 3, 70569 Stuttgart, Germany.

^b Department of Physics and Astronomy, Northern Arizona University, S San Francisco St., Flagstaff, AZ 86011, United States.

^c Institute for Physical Chemistry, University of Stuttgart, Pfaffenwaldring 55, 70569 Stuttgart, Germany.

† John.Gibbs@nau.edu

This work was supported in part by the Deutsche Forschungsgemeinschaft (DFG) as part of the project SPP 1726 (microswimmers, FI 1966/1-1).

Electronic Supplementary Information (ESI) available: Additional experimental procedures, results, methods and images in PDF format. Available videos: V1: Brownian motion bright field, V2 Brownian motion dark field, V3: circular swimming, V4: end over end, V5: translational only, V6: spinning only, V7: rotation suppression, and V8-12: example microdrills. See DOI: 10.1039/c000000x/

- Wang, J., *Nanomachines: fundamentals and applications*. John Wiley & Sons: 2013; Ebbens, S. J.; Howse, J. R., In pursuit of propulsion at the nanoscale. *Soft Matter* **2010**, *6* (4), 726-738; de Buyl, P.; Kapral, R., Phoretic self-propulsion: a mesoscopic description of reaction dynamics that powers motion. *Nanoscale* **2013**, *5* (4), 1337-1344.
- Bonin, K.; Kourmanov, B.; Walker, T., Light torque nanocontrol, nanomotors and nanorockers. *Optics Express* **2002**, *10* (19), 984-989; Jiang, H.-R.; Yoshinaga, N.; Sano, M., Active motion of a Janus particle by self-thermophoresis in a defocused laser beam. *Physical review letters* **2010**, *105* (26), 268302; Bregulla, A. P.; Yang, H.; Cichos, F., Stochastic Localization of Micro-Swimmers by Photon Nudging. *ACS nano* **2014**; Palacci, J.; Sacanna, S.; Steinberg, A. P.; Pine, D. J.; Chaikin, P. M., Living crystals of light-activated colloidal surfers. *Science* **2013**, *339* (6122), 936-940.
- Eelkema, R.; Pollard, M. M.; Vicario, J.; Katsonis, N.; Ramon, B. S.; Bastiaansen, C. W.; Broer, D. J.; Feringa, B. L., Molecular machines: Nanomotor rotates microscale objects. *Nature* **2006**, *440* (7081), 163-163; Li, J. J.; Tan, W., A single DNA molecule nanomotor. *Nano Letters* **2002**, *2* (4), 315-318.
- Wang, W.; Li, S.; Mair, L.; Ahmed, S.; Huang, T. J.; Mallouk, T. E., Acoustic Propulsion of Nanorod Motors Inside Living Cells. *Angewandte Chemie International Edition* **2014**, *53* (12), 3201-3204.
- Buttinoni, I.; Volpe, G.; Kümmel, F.; Volpe, G.; Bechinger, C., Active Brownian motion tunable by light. *Journal of Physics: Condensed Matter* **2012**, *24* (28), 284129.
- Sengupta, S.; Dey, K. K.; Muddana, H. S.; Tabouillot, T.; Ibele, M. E.; Butler, P. J.; Sen, A., Enzyme molecules as nanomotors. *Journal of the American Chemical Society* **2013**, *135* (4), 1406-1414.
- Loget, G.; Kuhn, A., Electric field-induced chemical locomotion of conducting objects. *Nature communications* **2011**, *2*, 535; Bricard, A.; Caussin, J.-B.; Desreumaux, N.; Dauchot, O.; Bartolo, D., Emergence of macroscopic directed motion in populations of motile colloids. *Nature* **2013**, *503* (7474), 95-98; Xu, X.; Liu, C.; Kim, K.; Fan, D., Electric-Driven Rotation of Silicon Nanowires and Silicon Nanowire Motors. *Advanced Functional Materials* **2014**.
- Ghosh, A.; Fischer, P., Controlled propulsion of artificial magnetic nanostructured propellers. *Nano letters* **2009**, *9* (6), 2243-2245; Pawashe, C.; Floyd, S.; Sitti, M., Modeling and experimental characterization of an untethered magnetic micro-robot. *The International Journal of Robotics Research* **2009**, *28* (8), 1077-1094; Vollmers, K.; Frutiger, D. R.; Kratochvil, B. E.; Nelson, B. J., Wireless resonant magnetic microactuator for untethered mobile microrobots. *Applied Physics Letters* **2008**, *92* (14), 144103.
- Lee, T.-C.; Alarcón-Correa, M.; Miksch, C.; Hahn, K.; Gibbs, J. G.; Fischer, P., Self-propelling nanomotors in the presence of strong Brownian forces. *Nano letters* **2014**, *14* (5), 2407-2412.
- Sánchez, S.; Soler, L.; Katuri, J., Chemically Powered Micro-and Nanomotors. *Angewandte Chemie International Edition* **2014**.
- Howse, J. R.; Jones, R. A.; Ryan, A. J.; Gough, T.; Vafabakhsh, R.; Golestanian, R., Self-motile colloidal particles: from directed propulsion to random walk. *Physical review letters* **2007**, *99* (4), 048102; Baraban, L.; Tasinkevych, M.; Popescu, M.; Sanchez, S.; Dietrich, S.; Schmidt, O., Transport of cargo by catalytic Janus micro-motors. *Soft Matter* **2011**, *8* (1), 48-52; Brown, A.; Poon, W., Ionic effects in self-propelled Pt-coated Janus swimmers. *Soft matter* **2014**, *10* (22), 4016-4027.
- Gibbs, J.; Zhao, Y.-P., Autonomously motile catalytic nanomotors by bubble propulsion. *Applied Physics Letters* **2009**, *94* (16), 163104-163104-3.
- Fournier-Bidoz, S.; Arsenault, A. C.; Manners, I.; Ozin, G. A., Synthetic self-propelled nanomotors. *Chemical Communications* **2005**, (4), 441-443; Paxton, W. F.; Sen, A.; Mallouk, T. E., Motility of catalytic nanoparticles through self-generated forces. *Chemistry-A European Journal* **2005**, *11* (22), 6462-6470; Qin, L.; Banholzer, M. J.; Xu, X.; Huang, L.; Mirkin, C. A., Rational design and synthesis of catalytically driven nanomotors. *Journal of the American Chemical Society* **2007**, *129* (48), 14870-14871.
- Mei, Y.; Solovev, A. A.; Sanchez, S.; Schmidt, O. G., Rolled-up nanotech on polymers: from basic perception to self-propelled catalytic microengines. *Chemical Society Reviews* **2011**, *40* (5), 2109-2119; Sanchez, S.; Ananth, A. N.; Fomin, V. M.; Viehrig, M.; Schmidt, O. G., Superfast motion of catalytic microjet engines at physiological temperature. *Journal of the American Chemical Society* **2011**, *133* (38), 14860-14863; Sánchez, S.; Xi, W.; Solovev, A. A.; Soler, L.; Magdanz, V.; Schmidt, O. G., Tubular Micro-nanorobots: Smart Design for Bio-related Applications. In *Small-Scale Robotics. From Nano-to-Millimeter-Sized Robotic Systems and Applications*, Springer: 2014; pp 16-27.
- Huang, W.; Manjare, M.; Zhao, Y., Catalytic Nanoshell Micromotors. *The Journal of Physical Chemistry C* **2013**, *117* (41), 21590-21596.
- Gibbs, J.; Kothari, S.; Saintillan, D.; Zhao, Y.-P., Geometrically designing the kinematic behavior of catalytic nanomotors. *Nano letters* **2011**, *11* (6), 2543-2550.
- Hawkeye, M. M.; Brett, M. J., Glancing angle deposition: fabrication, properties, and applications of micro-and nanostructured thin films. *Journal of Vacuum Science & Technology A* **2007**, *25* (5), 1317-1335.
- He, Y.; Wu, J.; Zhao, Y., Designing catalytic nanomotors by dynamic shadowing growth. *Nano letters* **2007**, *7* (5), 1369-1375.
- Purcell, E. M., Life at low Reynolds number. *Am. J. Phys* **1977**, *45* (1), 3-11.
- Solovev, A. A.; Xi, W.; Gracias, D. H.; Harazim, S. M.; Deneke, C.; Sanchez, S.; Schmidt, O. G., Self-propelled nanotools. **2012**.